# Constraining Sommerfeld enhanced annihilation cross-sections of dark matter via direct searches

Chiara Arina *, François-Xavier Josse-Michaux, Narendra Sahu

*Service de Physique Théorique, Université Libre de Bruxelles, 1050 Brussels, Belgium*

A B S T R A C T

In a large class of models we show that the light scalar field responsible for the Sommerfeld enhancement in the annihilation of dark matter leads to observable direct detection rates, due to its mixing with the standard model Higgs. As a result the large annihilation cross-section of dark matter at present epoch, required to explain the observed cosmic ray anomalies, can be strongly constrained by direct searches. In particular Sommerfeld boost factors of order of a few hundred are already out of the CDMS-II upper bound at 90% confidence level for reasonable values of the model parameters.

© 2010 Elsevier B.V. All rights reserved.

## 1. Introduction

Strong evidences support the existence of Dark Matter (DM) in the present Universe [1], although its actual nature is still missing. Identifying the DM is a major challenge for particle physics and has lead to a vast literature on extensions of the Standard Model (SM), in which many new particles comply with the requirements that a DM should fulfill. Over the last years, many efforts have been dedicated in building models of DM which leave signatures via direct and/or indirect detection.

A huge excitement in the indirect detection of DM took place after the PAMELA Collaboration [2] reported an unexpected rise in the positron fraction at energies from 10 GeV up to 100 GeV. Moreover, the H.E.S.S. [3] and Fermi Large Area Telescope [4] (FermiLAT) Collaborations reported an excess in the electron plus positron flux at energies above 100 GeV up to 1 TeV. If the DM is indeed the source of these observed anomalies in cosmic rays, then for a stable DM the current annihilation cross-section should be boosted by a factor of $\mathcal{O}(10^3)$ with respect to the freeze-out annihilation cross-section: $\langle \sigma_{\mathrm{DM}} |v| \rangle \approx 3 \times 10^{-26}$ cm$^3$ s$^{-1}$. An attractive way of getting a large enhancement of this cross-section without affecting the DM relic abundance is to invoke the Sommerfeld effect [5].

Recently CDMS-II [6] has reported two events in the signal region at 1.64 $\sigma$ confidence level (C.L.). The Collaboration has conservatively set an upper bound on the DM spin-independent cross-section on nucleon.

Typically indirect and direct detections of DM probe different sectors of parameter space of a model and have been studied as separate issues in the literature. In this Letter we consider the broad class of model where a light scalar $\phi$ is responsible for the Sommerfeld enhancement [7–11]. In these models we show that there exists a tight connection between direct and indirect detection of DM. Indeed the coupling responsible for the Sommerfeld enhancement also appears in the spin-independent cross-section on nucleon, in a unique combination with the Higgs portal coupling ($\phi$–$H$ mixing, $H$ being the Standard Model Higgs) as shown in Fig. 1, Refs. [11–14]. We demonstrate that from the direct detection bounds it is possible to set limits on the Sommerfeld enhancement that can arise at present epoch. Alternatively, for a given Sommerfeld enhancement, the Higgs portal coupling is strongly constrained [12,15] and can be probed at next generation direct detection experiments.

## 2. Light scalar–Higgs mixing

Considering that the DM candidate $\chi$ is a SM singlet fermion with mass $M_\chi$, stabilized by a $Z_2$ symmetry, and that the field $\phi$ is a real singlet scalar, the relevant terms in the Lagrangian are:

* Corresponding author.
*E-mail addresses:* carina@ulb.ac.be (C. Arina), fxjossemichaux@gmail.com (F.-X. Josse-Michaux), Narendra.Sahu@ulb.ac.be (N. Sahu).
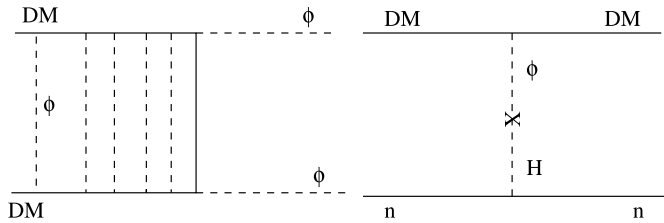
**Fig. 1.** A schematic presentation of the role of the light scalar field $\phi$ in indirect (left) and direct (right) detection of DM.

$$-\mathcal{L} \supset \lambda_\chi \overline{\chi^c} \chi \phi + \mu_\phi \phi H^\dagger H. \tag{1}$$

Once $H$ develops a non-zero vacuum expectation value (vev) $v$, $H$ and $\phi$ mix through the trilinear term $\propto \mu_\phi v$, $v = 246$ GeV. Due to $H$–$\phi$ mixing, the scalar field $\phi$ is unstable and ultimately decays to SM fields. Since $\phi$ is produced in the current DM annihilation, we demand $m_\phi \lesssim 1$ GeV in order to avoid the antiproton problem. Moreover, in order not to spoil the Big Bang Nucleosynthesis (BBN) predictions the thermally generated $\phi$ particles should disappear before the onset of the BBN, thus requiring $m_\phi > 10$ MeV [16,17]. It is true that for a DM candidate with mass in the 100 GeV–1 TeV range, such a low mass scale of $\phi$ may appear somewhat unnatural, being up-lifted by radiative corrections. A supersymmetric realization could however naturally solve this problem. In this Letter, without addressing this issue, we assume $m_\phi$ to be stabilized at the $\mathcal{O}(1)$ (GeV) scale.

Considering the Lagrangian in Eq. (1), the connection between the direct detection and the Sommerfeld enhancement is schematically presented in Fig. 1, with a key role played by $\phi$. The trilinear coupling $\lambda_\chi \overline{\chi^c} \chi \phi$ gives rise to an attractive Yukawa potential between $\chi$ particles, thus enhancing the current annihilation of $\chi \overline{\chi^c} \to \phi\phi$. The same coupling is also responsible for a spin independent interaction of $\chi$ with the nucleon $n$ through the Higgs portal coupling $\mu_\phi$. We express this coupling in terms of the mixing angle between $H$ and $\phi$, $\theta_{H\phi} \sim \mu_\phi v/(m_H^2)$, where $m_H$ is the physical Higgs mass in the SM. The mixing angle is lower bounded $\theta_{H\phi} \gtrsim 10^{-7}/\sqrt{m_\phi/\text{ GeV}}$ by demanding that the lifetime of $\phi$ should be less then $\tau_{\text{BBN}} \sim 1$ s [16,17]. The scalar field $\phi$ is indeed thermally produced in the early Universe and should decay before the onset of the primordial nucleosynthesis to avoid dominating the energy density of the Universe [12]. For the mass range of $\phi$ we consider, the mixing between $\phi$ and $H$ is also upper bounded, $\theta_{H\phi} < 10^{-2}$ [18].

The terms in Eq. (1) are ubiquitous in hidden sector models. The same Lagrangian arises in the case of $\phi$ being a complex singlet and developing a vev. The vector DM and the scalar DM cases are very similar to the fermionic example, although the presence of extra couplings may modify the phenomenology of the model. If a dark sector is gauged under a hidden symmetry, either Abelian or non-Abelian, then the DM may be constituted by the additional vector gauge boson of the theory [13,19]. Typically, SM fields are singlets under the hidden symmetry. For both Abelian and non-Abelian cases, the extra gauge bosons will couple to the light scalar $\phi$ through the kinetic term $|(\partial_\mu - ig_H T^a A'^a_\mu)\phi|^2$, $\phi$ being non-singlet under the hidden gauge group. The fermionic DM case then just translates to the gauge boson one by replacing $\lambda_\chi$ with the hidden sector gauge coupling $g_H$. In the non-Abelian case a kinetic mixing term between the SM hypercharge and the hidden gauge sector can arise from higher order operators. In this case interesting signatures arise [12,20]. In the case the DM is a complex scalar field $S$ in the hidden sector, the generality of our argument is somewhat weakened due to the presence of the additional coupling $f_{HS} S^\dagger S H^\dagger H$. The DM directly communicates to the SM sector through its Higgs portal coupling. Thus there is an additional channel in the DM to nucleon scattering, mediated by the SM Higgs through $t$-channel. Due to the presence of $f_{HS}$, the connection is more involved with respect to fermionic and vectorial cases and will be discussed elsewhere [21].

## 3. Sommerfeld enhancement

In the present case, the Sommerfeld enhancement is provided by the light scalar field $\phi$, which acts as a long range attractive force carrier between the $\chi$ particles. For a review on the Sommerfeld effect due to a light scalar field, see Ref. [7], while for non-Abelian massive vector fields one can see Ref. [22]. We define the coupling constant between the DM and $\phi$ as $\alpha_\chi = \lambda_\chi^2/(4\pi)$. When the Compton wavelength $\mathcal{O}(m_\phi^{-1})$ associated with $\phi$ becomes larger than $(\alpha_\chi M_\chi)^{-1}$, the asymptotic plane wave $\psi$ associated with $\chi$ gets distorted. The distortion can be computed by solving the Schrödinger equation for the attractive Yukawa potential $V(r) = -(\alpha_\chi/r)e^{-m_\phi r}$ and is defined as $S_e = |\psi(\infty)/\psi(0)|^2$ [7,22]. This is equivalent, in terms of Feynman diagrams, to the resummation of the multi-loop scalar ladder contributions, as shown in Fig. 1, the left diagram. The boost factor $S_e$ is a function of the dimensionless parameters $\epsilon_\phi = m_\phi/(M_\chi \alpha_\chi)$ and $\epsilon_v = \beta/\alpha_\chi$ only, with $\beta = v_{\text{rel}}/c$, the relative velocity between the DM particles.

By considering $S_e$ in a halo, we need to integrate over the relative velocity distribution of the DM halo [7,23]. Assuming an isothermal Maxwellian distribution with a mean velocity $v_0$, the averaged value of $S_e$ reads:

$$\langle S_e \rangle = \frac{4}{\sqrt{\pi}} \left( \frac{\alpha_\chi c}{v_0} \right)^3 \int_0^\infty d\epsilon_v \, \epsilon_v^2 e^{(-\epsilon_v^2 \alpha_\chi^2 c^2/v_0^2)} S_e(\epsilon_v, \epsilon_\phi). \tag{2}$$

It is a function of $\epsilon_\phi$ and $v_0/(c\alpha_\chi)$ only. We neglect the truncation of the Maxwellian distribution, since the cut-off on the escape velocity does not significantly affect the results. Indeed the enhancement drops rapidly with increasing velocities. The corresponding iso-contours of $\langle S_e \rangle$ are shown in Fig. 2. For small values of $v_0/(\alpha_\chi c)$ the boost factor can rise up to $10^4$, while for large $v_0/(\alpha_\chi c)$ the boost decreases down to 1.

Galactic cosmic rays, being measured by indirect DM search experiments, could arise from the current annihilation of DM. As a result PAMELA and Fermi experiments give upper bounds on the present DM total annihilation cross-section from the measurement of $e^{+/-}$ and $p$–$\bar{p}$ fluxes. For a DM mass ranging from 100 GeV to 1 TeV, the boost factor can be allowed up to a factor $\mathcal{O}(1000)$. Interestingly, as we see below, these boost factors suffer stringent constraints from direct detection exclusion limits.

## 4. Direct detection

The light scalar $\phi$ is the only field responsible for the DM scattering on nucleon due to its mixing with the SM Higgs. The elastic cross-section on nucleon, mediated by $\phi$ through $t$-channel, is given by:

$$\sigma_n^{SI} = \frac{\mu_n^2 f_n^2 m_n^2}{4\pi v^2} \frac{\lambda_\chi^2 \theta_{H\phi}^2}{m_\phi^4}, \tag{3}$$

where $\mu_n$ is the reduced nucleon–DM mass, $f_n = 0.3$, the effective Higgs nucleon interaction. The behavior of $\sigma_n^{SI}$ is driven by $1/m_\phi^4$. For a mass of $\phi$ in the MeV–GeV range, this cross-section can exceed the current upper bound on the elastic cross-section given by CDMS-II. The lighter the $\phi$ is, the smaller is the mixing angle required to be compatible with direct DM searches.
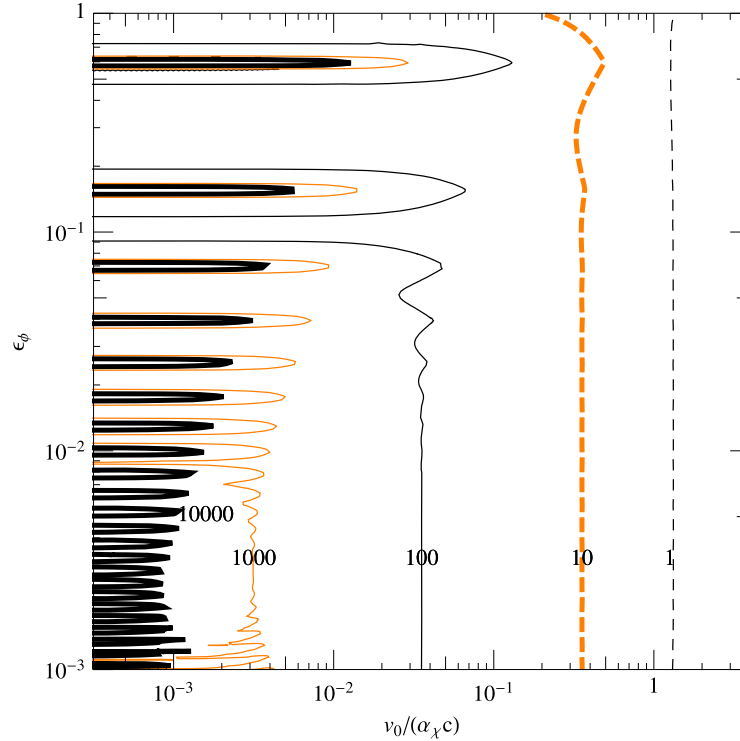
**Fig. 2.** Iso-contours of the non-perturbative Sommerfeld enhancement, $\langle S_e \rangle$, as a function of $v_0/(\alpha_\chi c)$ and $\epsilon_\phi$.

Actually what is measured in a terrestrial DM detector is the differential rate of nuclear recoils, integrated over the energy range of the experiment. This quantity is a function of the inverse mean velocity of the DM particles that can deposit a given recoil energy $E_r$. For details about the total rate the reader is referred to [24] and the references therein. With respect to the parameters used to define $\langle S_e \rangle$, the differential rate can be rewritten as:

$$\frac{dR}{dE_r} \propto \frac{\mu_n^2 f_n^2 m_n^2}{v^2} \frac{\lambda_\chi^2 c}{4\pi v_0} \frac{\theta_{H\phi}^2}{m_\phi^4} \frac{1}{y} F(x, y, z). \tag{4}$$

The function $F$ depends on the minimum velocity to produce a given recoil energy $x = v_{\min}/v_0$, the observed velocity $y = v_{\text{obs}}/v_0$ and the escape velocity $z = v_{\text{esc}}/v_0$. The observed velocity takes into account the motion of the Earth around the Sun. Typically, for an isothermal Maxwellian halo the range of values are 170 km/s $< v_0 < 270$ km/s [25] and 498 km/s $< v_{\text{esc}} < 608$ km/s [26]. The total rate is sensitive to the values of the escape velocity, the mean velocity and the minimum velocity, which depends on the DM mass, $E_r$ and the nucleus mass.

We consider only the CDMS-II exclusion limit since it is the most sensitive one in the DM range we are interested in (10 GeV–1 TeV). The Xenon10 [27] is most sensitive in the range 7–20 GeV. The experimental upper bound is obtained with the maximum gap method [28] and is given at 90% C.L.

## 5. Results and discussions

We begin by presenting our results for a mean velocity $v_0$ of the DM particles in the Earth's neighborhood of 220 km/s and an escape velocity of 600 km/s. The $\langle S_e \rangle$ is therefore a function of the coupling $\lambda_\chi$ and $m_\phi/M_\chi$. In each graph two suitable values of the mixing angle $\theta_{H\phi}$ are taken into account, depending on the $\phi$ mass.

In Fig. 3 we draw the iso-contours of the Sommerfeld boost factor and the exclusion limits from CDMS-II for $m_\phi = 0.1$ GeV (black curves) and 1 GeV (red curves), as labeled in the caption. For $0.1 \leqslant \lambda_\chi \leqslant 1.2$, boost factors ranging from 1 up to 1000 can be obtained, the right range to account for the PAMELA and Fermi $e^{+/-}$ and $p$–$\bar{p}$ measurements. However these values of $\lambda_\chi$ are strongly constrained by direct detection limits on DM–nucleon cross-section. For example, if $m_\phi = 0.1$ GeV, $M_\chi = 100$ GeV and $\theta_{H\phi} = 10^{-6}$ then only small values of $\lambda_\chi$ are allowed, namely $\lambda_\chi \lesssim 0.3$. Conversely, the maximum mixing angle allowed from direct detection can be inferred, down to $10^{-5}(10^{-3})$ for $m_\phi = 0.1$ GeV(1 GeV).

In Fig. 4 the iso-contours of the Sommerfeld enhancement are depicted and overlapped with the bounds from CDMS-II, for a fixed DM mass of 100 GeV. We can infer the allowed boost factor as follows. We see that $\theta_{H\phi} = 10^{-6}$ still allows $\langle S_e \rangle > 500$ for value of $m_\phi > 0.5$ GeV. A mixing angle of $10^{-4}$ excludes the possibility of having boost factor larger than 10. Had we increased the DM mass towards 1 TeV the direct searches would have been less sensitive. This is due to the huge difference in mass between the DM particle and the nucleus. For example, the CDMS-II detector is made of Ge ($m_{\text{Ge}} \sim 73$ GeV), hence the most sensitive region is around 50–100 GeV in mass.

The effect of the velocity on the exclusion limits and on the Sommerfeld enhancement is better understood in terms of the rescaled coupling $\lambda_\chi \sqrt{c/v_0}$. As shown in Fig. 2, $\langle S_e \rangle$ is indeed only dependent on the rescaled coupling. Variations of $v_0$ and $v_{\text{esc}}$ only affect the direct detection rate through the $F(x, y, z)/y$ factor, see Eq. (4). This modification is plotted in Fig. 5 for the extremal parameters $v_0 = 170$ km/s and $v_{\text{esc}} = 500$ km/s (red dotted and black long dashed lines) with respect to the reference values $v_0 = 220$ km/s and $v_{\text{esc}} = 600$ km/s (red dashed and black solid curves). This time we fixed $m_\phi = 0.1$ GeV. The change in direct detection sensitivity may be interpreted as a different value of the mixing angle saturating the current experimental upper bounds. Larger values of the mixing angle are indeed permitted.
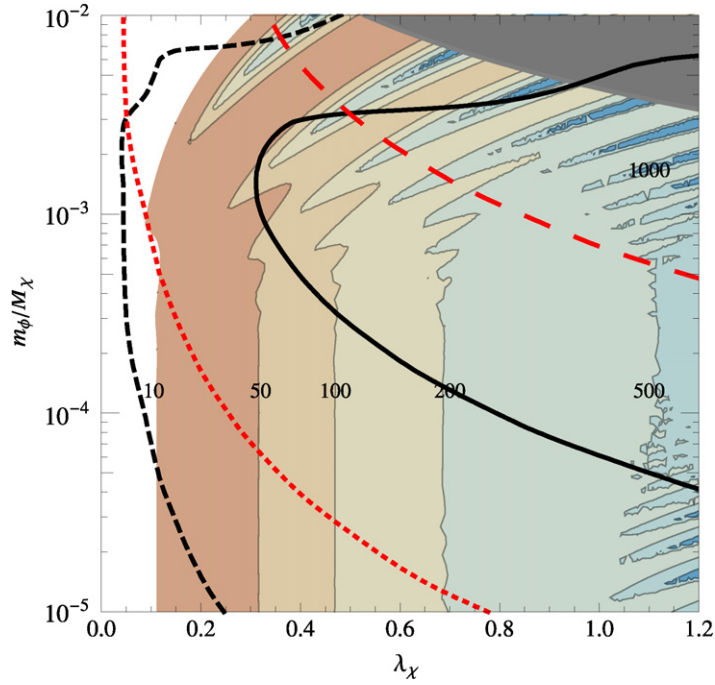
**Fig. 3.** Iso-contour of the Sommerfeld enhancement as a function of the coupling $\lambda_\chi$ and the ratio of the masses $m_\phi/M_\chi$. The thick black solid and dashed curves are the exclusion limits from CDMS-II for a mixing angle $\theta_{H\phi} = 10^{-6}$ and $\theta_{H\phi} = 10^{-5}$ respectively, with $m_\phi = 0.1$ GeV. In analogy the thick red long dashed and dotted lines are for $m_\phi = 1$ GeV and $\theta_{H\phi} = 10^{-4}$ and $\theta_{H\phi} = 10^{-3}$ respectively. The right-hand side of each curve is excluded at 90% C.L. The gray region is excluded by BBN, Eq. (6), for $m_\phi = 0.25$ GeV. (For interpretation of the references to color in this figure legend, the reader is referred to the web version of this Letter.)
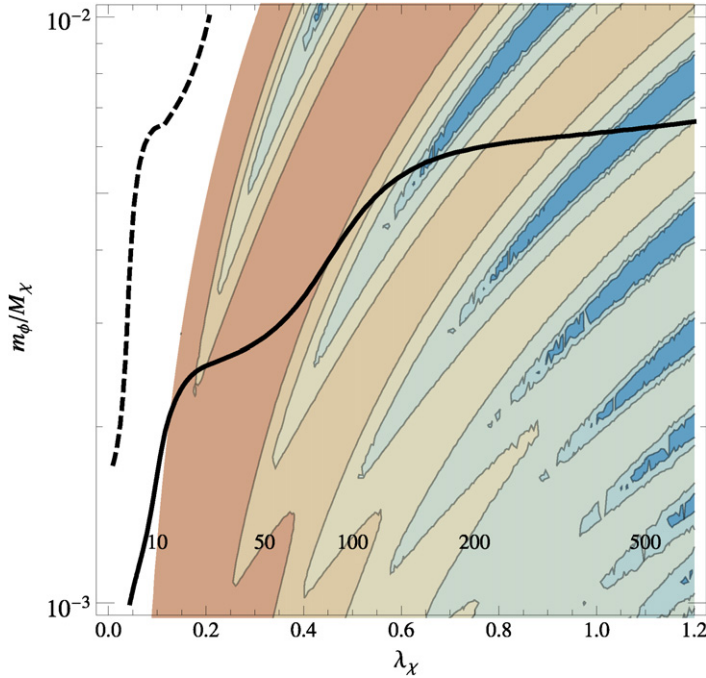


**Fig. 4.** Iso-contours of the Sommerfeld enhancement as a function of the coupling $\lambda_\chi$ and the ratio of the masses $m_\phi/M_\chi$ for a fixed DM mass $M_\chi = 100$ GeV. The thick solid and dashed black curves are the exclusion limits from CDMS-II for a mixing angle $\theta_{H\phi} = 10^{-6}$ and $\theta_{H\phi} = 10^{-4}$ respectively. The region below the curves is excluded at 90% C.L.

For $M_\chi = 10$ GeV and $\theta_{H\phi} = 10^{-5}$, the whole range of $\lambda_\chi$ (red dotted curve) is allowed for the extremal velocity parameters, while being upper bounded in the standard case (red dashed line). For $\theta_{H\phi} = 10^{-6}$ (black curves) and $M_\chi = 1000$ GeV, $\lambda_\chi = 1.2$ is still permitted for the extremal velocity values, implying viable boost factors up to 500 (long dashed), while from the reference case (solid) the allowed boost is at most of 200. In other words for a

given $\theta_{H\phi}$ the maximum allowed $\lambda_\chi$ and boost factor can be inferred. Although the constraints from direct detection are slightly reduced for smaller $v_0$ and $v_{\rm esc}$, the main results still hold.

Notice that we have implicitly assumed an isothermal Maxwellian velocity distribution for describing both the Earth's neighborhood (direct detection) and the galactic DM halo ($\langle S_e \rangle$). Our results however hold even in the presence of clumpy structures in the DM
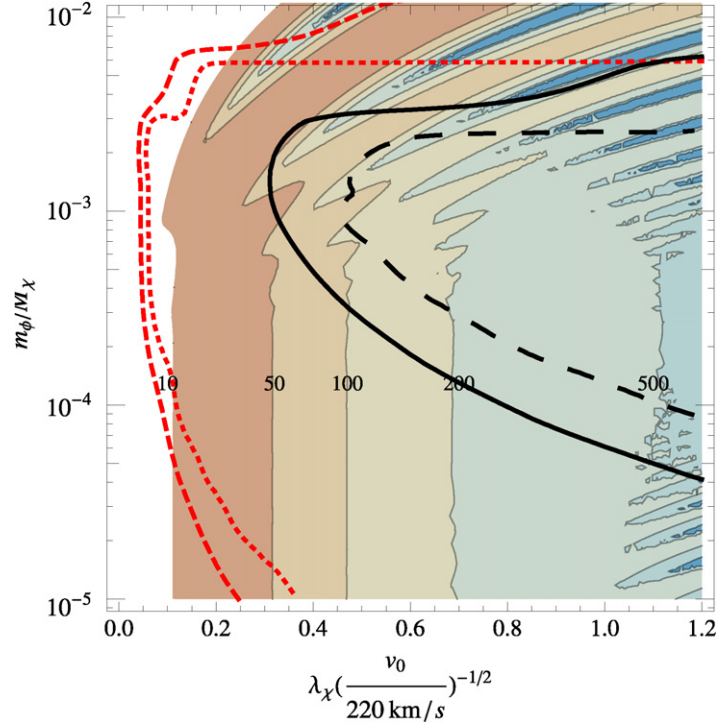
**Fig. 5.** Iso-contours of $\langle S_e \rangle$ as a function of the coupling $\lambda_\chi/\sqrt{v_0/(220 \text{ km/s})}$ and the ratio of the masses $m_\phi/M_\chi$ for a fixed $\phi$ mass of 0.1 GeV. The black solid and long dashed lines are for $\theta_{H\phi} = 10^{-6}$ and two different velocity parameters: $v_0 = 220$ km/s, $v_{\text{esc}} = 600$ km/s and $v_0 = 170$ km/s, $v_{\text{esc}} = 500$ km/s respectively. The same for the dashed and dotted red curves with $\theta_{H\phi} = 10^{-5}$. The right-hand side of the curves is excluded at 90% C.L. (For interpretation of the references to color in this figure legend, the reader is referred to the web version of this Letter.)

density profile. In that case, from Fig. 5, we see that the Sommerfeld boost factor is shifted by an amount $\sqrt{v_0^{\text{iso}}}/\sqrt{v_0^{\text{clump}}}$, where $v_0^{\text{clump}} \sim 14$ km/s. As a result higher boost factors become compatible with the direct detection.

When the DM interacts with the nucleus at a typical mean velocity $v_0/c \sim 10^{-3}$, a multi-loop scalar diagrams, as in Fig. 1, is also present. Potentially it can boost the direct detection rate as it does for the annihilation cross-section. With respect to the case of DM annihilation the bound state forms between the $\chi$ particle and the nucleus, when they have comparable masses [29]. The attractive Yukawa potential of the light scalar field is proportional to $\lambda_\chi \theta_{H\phi} f_n m_n/(4\pi v)$, due to the mixing with the Higgs boson. The effective coupling giving rise to the enhancement is suppressed with respect to $\alpha_\chi$ by the small Higgs nucleon coupling and the mixing angle is $\alpha_{DD} \sim 10^{-8}$ for $\theta_{H\phi} \sim 10^{-3}$. In term of $\langle S_e \rangle$, from Fig. 2, this correspond to large values of $v_0/(\alpha_\chi c)$. Thus no sizable boost factors are expected in this case.

We conclude this section with a remark on the relic density of the DM candidate $\chi$ and its link with the Sommerfeld boost factor [30] by assuming that the only interactions are given in Eq. (1). Then the total annihilation cross-section of $\chi$ can be estimated as:

$$\langle \sigma_\chi |v_{\text{rel}}| \rangle \approx \frac{\pi \alpha_\chi^2}{M_\chi^2} \times \left(1 + \frac{\theta_{H\phi}^2}{2}\right) + \frac{\alpha_\chi \mu_\phi^2}{M_\chi^4}. \tag{5}$$

Since the mixing angle $\theta_{H\phi} \propto \mu_\phi$, the second and third terms, which give the annihilation cross-section of $\chi$ particles into $H\phi$ and $H^\dagger H$, are suppressed for small mixing angles. As a result the first term dominates, which gives the annihilation cross-section of $\chi\chi \to \phi\phi$ through the $\chi$ exchange in $t$-channel. Hence from the relic abundance of DM, $\Omega_{\text{DM}} h^2 \sim 0.1$, one infers $\lambda_\chi \sim 0.6$ for $M_\chi \sim 1$ TeV, which is in the expected range of values that give large Sommerfeld enhancement as well as detectable elastic cross-

section on nucleon. However, this conclusion does not hold if the $\chi$ particles dominantly annihilate via some other channels in the early universe.

Even after the freeze-out of the DM, a small amount of $\chi$ pairs continue to annihilate with enhanced rate because of the Sommerfeld effect. The increased cross-section may disrupt the $^4$He and D abundances, which are benchmark predictions of the BBN. In our case the dominant diagram is the $t$-channel $\phi$ production, first term in Eq. (5): $\chi\chi \to \phi\phi$. The $\phi$ subsequently decays mainly into muons, due to its mass range. Assuming that BR$(\phi \to \mu^+\mu^-)$ is 100%, the photodissociation of the helium and deuterium abundances leads to an upper bound on the Sommerfeld coupling $\lambda_\chi$ [10,17]:

$$\lambda_\chi \lesssim 0.05 \times \left(\frac{M_\chi}{\text{GeV}}\right)^{3/4} \left(\frac{E_{\text{vis}}/M_\chi}{0.7}\right)^{-1/4}, \tag{6}$$

where $E_{\text{vis}}$ is the energy transferred to the visible sector. Notice that this constraint neither depends on the mixing angle nor on the $\phi$ mass. For a DM mass of 25 GeV, the maximum allowed $\lambda_\chi$ is 0.5, while for $M_\chi = 100$ GeV $\lambda_\chi = 2.5$. The BBN is capable to set a lower bound on the Higgs portal coupling and moreover for lower DM masses to strongly constraint the Sommerfeld enhancement. In Fig. 3 the gray region denotes the parameter space excluded by BBN, assuming $m_\phi = 0.25$ GeV. For larger DM masses, starting from 50 GeV, the CDMS-II experiment sets the stringent bounds on the allowed boost factors, while BBN constraints are relaxed in the range of values of $\lambda_\chi$ we consider.

At present epoch DM is annihilating in the galactic halo producing charged leptons, with an enhanced rate with respect to the freeze-out rate, due to the Sommerfeld mechanism. An increased neutrino flux can be detected at neutrino telescopes, which will constraint the boost factor [31] together with direct searches.

## 6. Conclusions

In this Letter we analyzed the connection between direct and indirect DM searches in a class of model where a light scalar field is added to the SM through a Higgs portal. This scalar acts as a long range force carrier and yields the Sommerfeld enhancement for the current annihilation of DM, as required by observed cosmic ray anomalies. The crucial point is that through $\phi$–$H$ mixing the light scalar allows the DM to scatter on nucleon, at rates possibly exceeding the exclusion limit of CDMS-II. In such scenarios the direct and indirect detections are fully determined only by $\lambda_\chi$, $\theta_{H\phi}$ and $m_\phi/M_\chi$. We found that a large part of the parameter space is strongly constrained in order to reconcile the current bounds from PAMELA and CDMS-II at 90% C.L.. For example using the $\phi$–$H$ mixing of order $10^{-6}$, $m_\phi = 0.1$ GeV and $M_\chi = 1$ TeV, the CDMS-II upper bound does not allow neither a boost factor of more than 200 nor $\lambda_\chi > 0.75$. While the interplay between direct and indirect detection is straightforward in the fermionic example we focused on, we stress that for all models where a light scalar is present and the DM candidate has zero SM hypercharge such an interplay does occur.

## Acknowledgements

## References

[1] G. Bertone, D. Hooper, J. Silk, Phys. Rept. 405 (2005) 279, arXiv:hep-ph/0404175;
G. Jungman, M. Kamionkowski, K. Griest, Phys. Rept. 267 (1996) 195, arXiv:hep-ph/9506380.
[2] O. Adriani, et al., arXiv:0810.4995 [astro-ph].
[3] F. Aharonian, et al., H.E.S.S. Collaboration, Phys. Rev. Lett. 97 (2006) 221102, arXiv:astro.ph/0610509;
F. Aharonian, et al., H.E.S.S. Collaboration, Phys. Rev. Lett. 97 (2006) 249901, Erratum;
F. Aharonian, et al., H.E.S.S. Collaboration, arXiv:0905.0105 [astro-ph].
[4] A.A. Abdo, et al., Fermi LAT Collaboration, arXiv:0905.0025 [astro-ph].
[5] A. Sommerfeld, Annalen der Physik 403 (1931) 257;
J. Hisano, S. Matsumoto, M.M. Nojiri, Phys. Rev. Lett. 92 (2004) 031303, arXiv:hep-ph/0307216.
[6] Z. Ahmed, et al., CDMS-II Collaboration, arXiv:0912.3592 [astro-ph.CO].
[7] N. Arkani-Hamed, D.P. Finkbeiner, T.R. Slatyer, N. Weiner, Phys. Rev. D 79 (2009) 015014, arXiv:0810.0713 [hep-ph].
[8] J.D. March-Russell, S.M. West, Phys. Lett. B 676 (2009) 133, arXiv:0812.0559 [astro-ph].
[9] M.R. Buckley, P.J. Fox, arXiv:0911.3898 [hep-ph];
W. Wang, Z. Xiong, J.M. Yang, L. Yu, JHEP 0911 (2009) 053, arXiv:0908.0486 [hep-ph];
Q. Yuan, et al., JCAP 0912 (2009) 011, arXiv:0905.2736 [astro-ph];
J. Mardon, Y. Nomura, J. Thaler, Phys. Rev. D 80 (2009) 035013, arXiv:0905.3749 [hep-ph];
H.S. Cheon, S.K. Kang, C.S. Kim, arXiv:0909.2130 [hep-ph];
Y. Bai, M. Carena, J. Lykken, Phys. Rev. D 80 (2009) 055004, arXiv:0905.2964 [hep-ph];
C. Balazs, N. Sahu, A. Mazumdar, JCAP 0907 (2009) 039, arXiv:0905.4302 [hep-ph].
[10] K. Kohri, J. McDonald, N. Sahu, Phys. Rev. D 81 (2010) 023530, arXiv:0905.1312 [hep-ph].
[11] D.P. Finkbeiner, T.R. Slatyer, N. Weiner, Phys. Rev. D 78 (2008) 116006, arXiv:0810.0722 [hep-ph].
[12] F. Chen, J.M. Cline, A.R. Frey, Phys. Rev. D 80 (2009) 083516, arXiv:0907.4746 [hep-ph].
[13] T. Hambye, JHEP 0901 (2009) 028, arXiv:0811.0172 [hep-ph].
[14] M. Pospelov, A. Ritz, M.B. Voloshin, Phys. Lett. B 662 (2008) 53, arXiv:0711.4866 [hep-ph];
Q.H. Cao, C.R. Chen, C.S. Li, H. Zhang, arXiv:0912.4511 [hep-ph];
N. Okada, O. Seto, arXiv:1002.2525 [hep-ph];
Y.G. Kim, K.Y. Lee, S. Shin, JHEP 0805 (2008) 100, arXiv:0803.2932 [hep-ph].
[15] Q.H. Cao, I. Low, G. Shaughnessy, arXiv:0912.4510 [hep-ph];
S.M. Carroll, S. Mantry, M.J. Ramsey-Musolf, Phys. Rev. D 81 (2010) 063507, arXiv:0902.4461 [hep-ph].
[16] M. Kawasaki, K. Kohri, T. Moroi, Phys. Rev. D 71 (2005) 083502.
[17] J. Hisano, M. Kawasaki, K. Kohri, T. Moroi, K. Nakayama, Phys. Rev. D 79 (2009) 083522, arXiv:0901.3582 [hep-ph].
[18] D. O'Connell, M.J. Ramsey-Musolf, M.B. Wise, Phys. Rev. D 75 (2007) 037701, arXiv:hep-ph/0611014.
[19] P.H. Gu, H.J. He, U. Sarkar, X. Zhang, Phys. Rev. D 80 (2009) 053004, arXiv:0906.0442 [hep-ph].
[20] C. Arina, T. Hambye, A. Ibarra, C. Weniger, JCAP 1003 (2010) 024, arXiv:0912.4496 [hep-ph].
[21] C. Arina, F.X. Josse-Michaux, N. Sahu, arXiv:1004.3953 [hep-ph].
[22] M. Cirelli, A. Strumia, M. Tamburini, Nucl. Phys. B 787 (2007), arXiv:0706.4071 [hep-ph].
[23] J. Bovy, Phys. Rev. D 79 (2009) 083539, arXiv:0903.0413 [astro-ph.HE].
[24] C. Savage, G. Gelmini, P. Gondolo, K. Freese, JCAP 0904 (2009) 010, arXiv:0808.3607 [astro-ph];
C. Arina, F.S. Lin, M.H.G. Tytgat, JCAP 0910 (2009) 018, arXiv:0907.0430 [hep-ph].
[25] C.S. Kochanek, Astrophys. J. 457 (1996) 228, astro-ph/9505068.
[26] M.C. Smith, et al., Mon. Not. Roy. Astron. Soc. 379 (2007) 755–772, astro-ph/0611671.
[27] J. Angle, et al., XENON10 Collaboration, Phys. Rev. D 80 (2009) 115005, arXiv:0910.3698 [astro-ph.CO].
[28] S. Yellin, Phys. Rev. D 66 (2002) 032005, arXiv:physics/0203002.
[29] T.R. Slatyer, JCAP 1002 (2010) 028, arXiv:0910.5713 [hep-ph].
[30] J.B. Dent, S. Dutta, R.J. Scherrer, Phys. Lett. B 687 (2010) 275, arXiv:0909.4128 [astro-ph.CO];
J.L. Feng, M. Kaplinghat, H.B. Yu, arXiv:0911.0422 [hep-ph];
J. Zavala, M. Vogelsberger, S.D.M. White, arXiv:0910.5221 [astro-ph.CO].
[31] C. Delaunay, P.J. Fox, G. Perez, JHEP 0905 (2009) 099, arXiv:0812.3331 [hep-ph].